Journal of Pharmaceutical Sciences 115 (2026) 104257

Contents lists available at ScienceDirect

Journal of Pharmaceutical Sciences

journal homepage: www.jpharmsci.org

Pharmaceutical Biotechnology

Comprehensive stress study on recombinant adeno-associated virus vectors: Evaluating the capabilities of established analytical techniques

Jakob Heckel[a,b,*], Lukas Bongers[b], David Naylor[c], Ole Schmidt[c], Raphael Ruppert[b], Marco Thomann[b], Florian Semmelmann[a], Angie Kirchner[d], Alexandra H.E. Machado[c], Markus Haindl[b], Michael Leiss[a], Jürgen Hubbuch[e], Tobias Graf[a]

[a] *Pharma Technical Development Analytics, Roche Diagnostics GmbH, 82377 Penzberg, Germany*
[b] *Pharma Technical Development Cell & Gene Therapy, Roche Diagnostics GmbH, 82377 Penzberg, Germany*
[c] *Pharma Technical Development, Pharmaceutical Development and Supplies EU, F.Hoffmann-La Roche AG, 4070 Basel, Switzerland*
[d] *Roche Pharma Research & Early Development, Roche Innovation Center Munich, Roche Diagnostics GmbH, 82377 Penzberg, Germany*
[e] *Institute of Process Engineering in Life Sciences, Section IV: Biomolecular Separation Engineering, Karlsruhe Institute of Technology, 76131 Karlsruhe, Germany*

ARTICLE INFO

Article history:
Received 14 November 2025
Revised 4 March 2026
Accepted 11 March 2026
Available online 18 March 2026

Keywords:
Gene therapy
Adeno-associated virus (AAV)
Viral vector
Physical characterization
Biopharmaceutical characterization
Physical stability
Chemical stability
Stability
Forced conditions

ABSTRACT

Recombinant adeno-associated virus (rAAV) vectors are prominent vectors for *in-vivo* gene therapies. However, achieving consistent product quality is a major challenge due to the inherent complexity of their structure and the associated production process. During manufacturing and storage, virus particles are exposed to a variety of stresses, which can have a direct impact on product attributes, thereby potentially also affecting safety and efficacy. Current understanding of stress-induced degradation for rAAVs is still fragmented, both on a mechanistic level and regarding the identification of the most appropriate analytical tools to detect the underlying changes. To address these gaps, the impact of different stress conditions, namely freeze-thaw, elevated temperature, high/low pH and light exposure, was tested on two different serotypes. For this, a comprehensive panel of orthogonal analytical methods was applied to identify significant changes in capsid and genome titer, full-to-total ratio, content of aggregates, payload integrity and post-translational modifications. By correlating this extensive dataset with potency results, this study provides detailed insights into the degradation behavior of the employed rAAVs and the suitability of state-of-the-art analytical techniques to indicate the stability of the product. Overall, substantial differences in stress responses were observed between the two serotypes investigated, and changes in transduction efficiency were mostly represented inadequately at the structural or molecular level by the analytical methods employed. Based on these findings, this study serves as a framework for refining the analytical control strategy of rAAV-based gene therapies and for developing robust, stability-indicating assays.

© 2026 The Author(s). Published by Elsevier Inc. on behalf of American Pharmacists Association®. This is an open access article under the CC BY-NC-ND license (http://creativecommons.org/licenses/by-nc-nd/4.0/)

Introduction

Recombinant adeno-associated virus (rAAV) vectors are frequently used delivery vehicles for *in-vivo* gene therapies, as they promise high tissue tropism and long-term gene expression with a positive benefit-risk profile.[1] rAAVs are icosahedral, non-enveloped viral particles belonging to the *Parvoviridae* family. The protein shell is 18-25 nm in diameter and encapsulates single-stranded DNA (ssDNA) carrying the gene of interest. rAAV-capsids comprise in total 60 copies of viral protein (VP) 1,2 and 3 with VP3 being the most abundant. Their assembly occurs in a stochastic manner, entailing the formation of a highly heterogenous population of capsids. In this regard, it has been estimated that the most abundant VP-assembly represents less than 2.5% of the total rAAV population.[2] In addition, the encapsulation process of the ssDNA payload is imperfect, often yielding a mixture of empty capsids and particles containing truncated or non-therapeutic genomes.[3] Due to their size and complexity, analytical quality control and extended characterization of rAAVs is highly demanding. Apart from the above-mentioned heterogeneity,

* Corresponding author at: Roche Diagnostics GmbH, Nonnenwald 2, 82377 Penzberg, Germany.
E-mail address: jakob.heckel@roche.com (J. Heckel).

https://doi.org/10.1016/j.xphs.2026.104257
0022-3549/© 2026 The Author(s). Published by Elsevier Inc. on behalf of American Pharmacists Association®. This is an open access article under the CC BY-NC-ND license (http://creativecommons.org/licenses/by-nc-nd/4.0/)

rAAVs encounter a variety of different stresses during manufacturing, formulation, storage and transport leading to chemical and physical degradation, which in turn can affect their biological activity.[4]

It is therefore of paramount importance to (i) identify stress conditions that can have a negative impact on the potency of rAAV vectors and (ii) develop appropriate analytical methods that can reliably detect these alterations at the structural or molecular level.

The importance of understanding and mitigating potential stresses on rAAVs was highlighted in a variety of recent studies. In this context, the most assessed factors were long-term storage and temperature stability including multiple freeze-thaw (FT) cycles as well as low pH conditions that occur during manufacturing and endosomal trafficking.[5–10] These studies report a broad spectrum of findings, ranging from negligible or minimal effects to significant degradation, depending on the specific conditions and factors involved. Ultimately, the critical quality attribute considered most relevant is biological activity, or potency, which is measuring the product's ability to produce the desired effect.[11] However, direct analysis of this CQA by means of potency assays is of limited practicality due to the inherent variability of these techniques usually relying on the quantification of a specific cellular response in multi-step protocols. In addition, these assays are generally restricted by their low throughput, impeding the realization of extensive stress studies. To address this bottleneck, the implementation of appropriate analytical methods that can resolve subtle structural or molecular changes is crucial. Optimally, such biophysical and physicochemical assays can serve as predictive surrogates for biological activity. By correlating these product attributes with potency, a structure-function relationship can be established, whose insights can then be used to promote efficient process development and robust quality control.

Despite recent publications investigating the impact of stress conditions on the integrity of rAAVs, the overall understanding of these effects and the identification of the most appropriate analytical methods to resolve stress-induced alterations is still limited. This is partly because most of the available studies focus on either one serotype or a specific stressor, and apply only a narrow panel of analytical techniques, thereby limiting the ability to draw comprehensive conclusions or establish a universal framework. To address this gap, we conducted a systematic assessment of multiple stress conditions, including freeze-thaw, elevated temperature, low and high pH, as well as mild and strong UV light, on two different AAV serotypes. For this, the capsid and vector genome titer as well as the formation of aggregates and fragments were analyzed with multiple complementary methods. In addition, payload integrity, the occurrence of post-translational modifications (PTMs) and the presence of free ssDNA, as well as additional product attributes when deemed helpful, were characterized by applying state-of-the-art analytical techniques. By comparing this extensive dataset with *in-vitro* potency results, we were able to identify the most critical degradation pathways and determine which analytical methods are most predictive of biological activity, ultimately proposing clear guidelines for stability testing and establishing a robust analytical strategy for quality control of rAAV gene therapy products.

Material and methods

All samples were prepared and stored using Protein LoBind® Tubes (Eppendorf SE, Hamburg, Germany) in sizes of 0.5, 1.5 and 15 mL.

Buffer 1 (neutral storage Buffer): 20 mM Tris, 200mM NaCl, 1mM $MgCl_2$, 0.005% Poloxamer 188, pH 7.95;

Buffer 2 (high pH): 20 mM Tris, 200 mM NaCl, 1mM $MgCl_2$, 0.005% Poloxamer, pH (before sample preparation) 10.58, target stress pH 9.2;

Buffer 3 (low pH):20 mM Citrate, 140 mM NaCl, 1mM $MgCl_2$, 0.005% Poloxamer, pH (before sample preparation) 2.88, target stress pH 3.0;

All buffer components were obtained from Merck (Merck KGaA, Darmstadt, Germany). Buffers were 0.22μm sterile filtrated and kept refrigerated at 4°C until their usage.

Serotypes

Two AAV serotypes were used throughout the stress experiments: wild-type AAV9 (wtAAV9) and an in-house produced AAV2-derived (rAAV2der) capsid. Both serotypes carry the identical DNA payload encoding the fluorescent protein mGreenLantern (mGL). The initial stocks were produced through triple-plasmid transfection of HEK293 cells in 500 L large scale culture. After 72h, cell culture fluid was harvested, the cells were lysed and the material was concentrated using UF/DF followed by affinity capture (rAAV2der) and subsequent ion-exchange chromatography to enrich full capsids (wtAAV9). The respective pools exhibited a full-to-total ratio (FTR) between 50% to 70%, ensuring that both empty and full capsids were represented sufficiently. Stock solutions were buffer exchanged with neutral storage buffer (Buffer 1) and concentrated to an initial concentration of 5×10^{14} cp/mL, as determined by ELISA. Aliquots were prepared and frozen at -80°C for subsequent use in stress experiments.

General setup of stress experiments

Sample preparation

For each experiment, a 1.1 mL stock aliquot was diluted with 4.4 mL of the designated stress buffer (Buffers 1, 2 or 3) to yield a final volume of 5.5 mL of AAV solution with a target titer of 1×10^{14} cp/mL. Homogeneity was ensured by pulse vortexing for 1 to 2 seconds. A negative effect of vortexing on sample stability for the investigated serotypes was excluded during pre-experiments. The resulting solution was then aliquoted into five distinct 1.5 mL Eppendorf Protein LoBind® tubes, each receiving 1.05 mL. Each tube represents one sampling point.

Different stress conditions were applied as described in the subsequent paragraphs. After stress application, each sample was vortexed briefly. Subsequently, 1 mL of the stressed sample was withdrawn, gravimetrically diluted with storage buffer (Buffer 1) to a final amount of 10 g, thus targeting a final titer of 1×10^{13} cp/mL), and vortexed again. The sample was aliquoted into 50, 100, 200 and 500 μL volumes for subsequent analysis and stored frozen at -80°C, adding one freeze-thaw cycle to each analyzed sample.

Additional buffer exchange for pH stressed samples

To prevent any influence of the pH stress buffers after completing the stress study, a buffer exchange was performed using 15 mL Amicon® Ultra Centrifugal Filters (Merck) with a 50 kDa molecular weight cut-off. 1 mL of the sample was pipetted into the filter tube and mixed with 14 mL of neutral storage buffer (Buffer 1). The sample was centrifuged for 30 minutes at 4°C and 2500 rpm. The retentate, typically less than 1 mL, was collected using a pipette. The filter was thoroughly washed twice with 2 mL of storage buffer to recover capsids from the filter tube and finally stocked up to a final amount of 10 g before aliquoting as described above.

Specific stress conditions

Freeze-thaw

For each complete freeze-thaw cycle, samples were directly transferred and without a controlled rate between a -80°C freezer, where

they were stored for at least 1 hour and an 8°C refrigerator, where they were thawed for 1 hour. Samples were drawn immediately after 1, 2, 5 and 10 cycles and processed as described. An additional reference sample ($cycle_0$) was aliquoted for analysis prior to the F/T stress and stored frozen at -80°C, representing a non-stressed control sample.

Temperature

Temperature stress was applied by placing samples in an incubator at 37°C (with humidity and CO_2 control turned off). Sampling was conducted after 2, 4, 8 and 14 days. A reference control sample (T_0) was placed in a fridge at 4°C for 14 days. All samples were wrapped in aluminum foil to avoid any exposure to light stress.

pH stress

In order to achieve the pH of 3.0 (low pH) and 9.2 (high pH), the aliquoted AAV stocks were diluted by a factor of 4 in the respective pH stress buffers (Buffers 2 and 3). Final pH was assessed and confirmed to be within the range of ± 0.1 pH units of the targeted pH. Four samples for each pH were placed in the fridge at 4°C. Two control samples were prepared by diluting the stock with neutral pH storage buffer (Buffer 1). While one control sample was directly buffer exchanged and aliquoted as described above ($pH_{neutral,\ start}$), the second control sample was placed in the fridge to account for potential sample alterations due to storage time in the fridge ($pH_{neutral,\ end}$).

Light stress

To investigate the photostability of AAV vectors, two different stress conditions (Mild Light and UV Light) were applied. Samples were filled in 2 mL Crystal Zenith® (CZ) vials (DAIKYO, Tochigi, Japan), stoppered and crimped before being placed horizontally in the respective light chambers at 25°C. For both approaches, a dark control sample (dc) was prepared by wrapping a CZ vial in aluminum foil and placing it in the light chamber as well. A 2 cm distance was kept between vials to ensure uniform and maximum light exposure. To monitor stress induced by the elevated temperature of 25°C, an additional control sample was aliquoted and frozen directly, representing a completely non-stressed sample without any application of light and temperature stress (L_0). Notably, initial aliquots and final samples were not vortexed during this experiment but mixed on a tube roller for 5 minutes at a moderate rolling intensity. UV stress was performed according to EMA guideline ICH Q1 by using a Suntest XLS light chamber (Ametek, Berwyn,PA) and exposing samples to 250 Wh/m^2 over the course of 24 h. For mild light stress, the CZ vials were placed in a Caron Photostability Chamber 6540 (Caron Scientific & Services, Marietta, OH). Light exposure time was set to 50 h with an irradiance of 0.1 W/m^2 UV light and 5 klx illuminance using a UV filtered cool white light fluorescence lamp to reflect the expected daylight irradiance and illuminance in a manufacturing area, adapting ICH Q1.

A comprehensive overview of the different stress and sampling conditions is summarized in Table 1.

Analytical assessment of quality attributes

Cell-based functional transduction assay

Potency was assessed by applying a cell-based *in-vitro* transduction assay. Human-derived cell lines were seeded into a tissue culture 96 well plate (Thermo Fisher Scientific, Waltham, MA) at a density of 50,000 cells/well in 200 μL Dulbecco's Modified Eagle Medium (Thermo Fisher Scientific) medium supplemented with 10% Fetal Bovine Serum. Cells were incubated at 37°C, 5% CO_2 and subsequently, the wells were transduced in nine distinct steps per sample with a multiplicity of infection (MOI) in a range of 0.6 to 200,000 based on the mean vg titer of the unstressed control samples as assessed by ddPCR. After 24 h incubation, the medium was aspirated and cells were detached by adding trypsin. After transferring to a V-bottom 96-well plate (Thermo Fisher Scientific), cells were centrifuged and washed with PBS twice prior to resuspending them in 150 μL of a buffer suitable for fluorescence activated cell counting (FACS). Plates were then analyzed using a FACSLyric flow cytometry instrument (BD Sciences, Franklin Lakes, NJ) detecting the intrinsic fluorescence of expressed mGL. Each sample was prepared in biological duplicates and transduction efficiency was calculated from the sigmoidal relationship between the MOI and the expression of the target protein, using the linear portion of the curve to determine potency.

Capsid and/or payload quantification

Antibody-based immunoassay (ELISA)

A commercially available sandwich ELISA assay was obtained to determine total capsid titer. Immobilized Capture Select™ biotinylated anti-AAVX conjugate (Thermo Fisher Scientific) was used to capture rAAV2der (respectively anti-AAV9 conjugate for wtAAV9). Following a washing step, Capture Select™ HRP anti-AAVX or AAV9 conjugate (Thermo Fisher Scientific) were employed as detection antibodies for capsid titer determination. Samples were diluted manually to fit the dynamic range of the assay, ranging in between 1×10^6 to 5×10^{10} cp/mL, with reported limit of detection (LOD) at 5×10^5 cp/mL, and each sample was measured in triplicates.[12,13]

Affinity-based high-performance liquid chromatography (HPLC)

POROS™ CaptureSelect™ AAVX or AAV9 resin (Thermo Fisher Scientific) was packed in small analytical columns (2 × 20 mm) and installed on an Agilent 1260 Infinity II OnlineLC system (Agilent, Santa Clara, CA) containing a UV diode array detector (DAD, G7117B) equipped with a 60 mm Max-Light Cartridge Cell (4 μL; G4212-60007) and a 1260 Infinity fluorescence detector (FDL, G1321B).

For each measurement, 10 μL of sample were injected on to the column followed by a short wash step to reduce sample impurities before elution. Depending on the rAAV serotype, sample injection volume and sensitivity settings of the fluorescence detector, the assay can quantify capsid titers within a range of 6×10^9 to 1.5×10^{14} cp/

Table 1
Experimental setup for the performed stress studies.

Stress	Condition	Sampling	Controls
Freeze-Thaw	-80°C/8°C	0, 1, 2, 5, 10 cycles	$cycle_0$
Temperature	37°C	2, 4, 8, 14 days	T_0
High pH	pH 9.2 at 4°C	2, 4, 8, 14 days	Shared controls: $pH_{neutral,\ start}$, $pH_{neutral,\ end}$
Low pH	pH 3.0 at 4°C		
Light	Mild light UV light	2 different conditions	L_0, $dc_{mild\ light}$, $dc_{UV\ stress}$

mL. Detection of the eluting peak was performed using UV absorbance (UV260 and UV280) and fluorescence detection (FLD), enabling the determination of both FTR and capsid titer.[14,15] Triplicates were assessed for each sample.

Size exclusion chromatography – multi angle light scattering (SEC-MALS)

SEC-MALS analysis was conducted using an Ultimate 3000 (Thermo Fisher Scientifc) HPLC equipped with Optilab ™ RI and microDAWN ™ MALS (Wyatt Technology, Santa Barbara, CA) detection modules. Samples were separated on a 300mm SRT SEC-500 column (Sepax Technologies, Newark, DE) using a pH neutral potassium chloride buffer. Samples were assessed as duplicates in separate sequences and ASTRA 8.1.2 was used for acquiring and analyzing UV, RI and MALS data. For dn/dc 0.185 mL/g and 0.170 mL/g were used for protein and nucleic acid, respectively. The expected molecular weight was calculated by the nucleic acid and protein sequences. As the UV extinction coefficients of payload DNA and capsid protein display only slight variation across different serotypes, generic values, as proposed by Wyatt, were applied.[16] More detailed descriptions of the method, including comprehensive insights into its physical principles, have been published elsewhere, indicating a reported limit of quantification (LOQ) of 2.5×10^{12} and respectively a LOD of 5×10^{11} cp/mL.[17,18]

Digital droplet polymerase chain reaction (ddPCR)

Initial free DNA was digested using a DNAse treatment, followed by proteinase K (Thermo Fisher Scientific) digest of the capsid and release of internal ssDNA payload. A short heat-treatment was applied for inactivation of enzymatic activity. Since the ddPCR method operates within a dynamic range of 5×10^1 to 6×10^6 copies/mL reaction volume, samples were diluted accordingly prior to vector genome (vg) titer assessment, which was done in triplicates. Droplets were generated using an AutoDG instrument (Bio-Rad Laboratories, Hercules, CA) and placed in a QX200 ddPCR system (Bio-Rad). Primers and fluorescence probes for the cytomegalovirus (CMV) promoter region of the employed mGL payload were used for PCR analysis. Evaluation using the Poisson distribution was applied on retrieved data to calculate the concentration of vg copies in each sample.[19]

Mass photometry (MP)

Samples were diluted in PBS to approximately 5×10^{11} cp/mL to ensure they fell within the reported linear detection range of 1×10^{11} to 8×10^{11} cp/mL. The samples were pipetted one at a time for each measurement into a 24-well cassette mounted upon a glass slide, which was placed above the laser in the SamuxMP instrument (Refeyn, Waltham, MA). 60-second videos of binding events were recorded for each sample and evaluated, utilizing the linear relation of mass and scattering signals, allowing the calculation of FTR as well as an estimation of partially filled capsids. All measurements were performed in triplicate with binding event counts between 500 to 6,000, ensuring at least 300 counts for either the empty or full capsid peaks. The LOQ of MP was reported at 8.8×10^{10} cp/mL.[20–22]

Fluorescent DNA staining

The Qubit™ ssDNA Assay-Kit (Thermo Fisher Scientific) was utilized for quantitation of free single-stranded DNA (ssDNA). According to the manufacturer, the assay has a calibration range of 1 to 1000 ng/mL and supports sample volumes of 1 to 20 μL, therefore enabling the analysis of sample concentrations ranging from 10ng/mL to 240 μg/mL. According to the instructions, 20 μL of each sample were mixed with 180 μL of reaction mix. After 2 minutes reaction time, ssDNA titer was measured using the Qubit™ 4 Fluorometer (Thermo Fisher Scientific).[23]

All samples were prepared and analyzed in technical triplicate. To additionally evaluate the total amount of ssDNA, samples underwent thermal payload ejection by heating to 70°C for 30 minutes, followed by sample dilution in a 1 to 12 ratio prior to measurement. The amount of free ssDNA was calculated based on the relative ratio of initial free ssDNA to complete ejected ssDNA after heat treatment. Heat-treated samples were analyzed in single measurements, while the mean total ssDNA amount for each serotype was derived from all tested samples.

Aggregation measurement

SEC-UV/FLD

SEC-UV/FLD runs were performed in duplicate as previously described (see SEC-MALS), utilizing UV detection at 280 nm and fluorescence detection (FLD) with excitation/emission wavelengths of 280/350 nm. The high sensitivity of fluorescence detection, combined with the intrinsic fluorescence of rAAV capsid proteins, allows the quantification of capsids down to a limit of 3.5×10^{11} cp/mL. By contrast, UV-based quantification is highly dependent on the proportion of payload containing capsids, as the high absorbance of DNA at 260 nm strongly interferes with measurements at 280nm, resulting in a LOQ as low as 8×10^{10} vg/mL.[24]

SEC-UV/FLD was primarily employed for the assessment of capsid aggregation, where the relative amount of High Molecular Weight species (HMWs), representing oligomeric aggregates, as well as Low Molecular Weight species (LMWs), such as fragmented capsids and free DNA, were determined based on the observed signals.[25]

Dynamic light scattering (DLS)

DLS was used to evaluate the hydrodynamic radius (rH) and size distribution of viral particles within the size ranges of 10-100 nm, corresponding to individual capsids or smaller HMWs, and 100-1000 nm, indicative of larger aggregates. For analysis, 30 μL of each sample was pipetted in triplicate into a 384-well plate, centrifuged for 1 minute at 400g to remove larger debris and placed into a DynaPro Plate Reader III (Wyatt). The hydrodynamic radius and the relative size distribution of capsids and aggregates were calculated based on the obtained autocorrelation functions.[26,27]

Molecular and structural analysis

Post-translational modifications (PTMs) by liquid chromatography – mass spectrometry (LC-MS)

Prior to analysis, capsids were denatured at 90°C for 20 min, followed by enzymatic digestion adding trypsin and incubation at 37°C for 20 h. A stop solution was added and samples were analyzed in triplicate using a Vanquish™ Flex UHPLC System (Thermo Fisher Scientific), equipped with a ACQUITY UPLC Peptide CSH C18 Column (Waters Corporation, Milford, MA) and coupled to an Orbitrap Exploris™ 240 mass spectrometer. MS1 data were evaluated using Byonics (Protein Metrics, Boston, MA) to calculate the relative amount of post-translational modifications (PTMs) at specific sites. All reported PTM sites are labeled according to their position following common VP1 nomenclature.

Negative-stain transmission electron microscopy (nsTEM)

The integrity of temperature- and light-stressed samples was evaluated by applying transmission electron microscopy (TEM) on endpoint and control samples for virtual comparison. For this procedure, 2 μL of sample was pipetted onto a carbon grid and incubated for 30 seconds followed by 15 seconds of uranyl acetate staining. Images were taken with a 50,000x magnification on a JEM-1400Plus (Jeol, Tokyo, Japan) electron microscope.

Next generation sequencing (NGS)

The AAV payload was extracted using the QIAamp® MinElute® Virus Spin Kit (Qiagen, Hilden, Germany). Double-strand synthesis, followed by repair, A-tailing and adapter ligation using the SMRTbell® prep kit 3.0 (PacBio) was performed according to the manufacturer's protocols with slight adjustments. The SMRTbell library was sequenced on a Sequel IIe instrument (Pacific Biosciences, Menlo Park, CA).

Capillary electrophoresis (CE)

CE-SDS analysis of viral protein capsid stoichiometry was conducted using the BioPhase 8800 (SCIEX, Framingham, MA) system equipped with a laser-induced fluorescence (LiF) detector. Separations were performed at 25°C using a 50 μm fused silica capillary (30 cm total length, 20 cm separation distance) under reverse polarity at 15 kV, with sample injection at 5.0 kV for 30 s. The capillary was pre-rinsed with NaOH, HCl, water, and SDS-MW matrix, and data were analyzed using Chromeleon™ 7.3.2 (Thermo Fisher Scientific).

Statistical evaluation

To assess the methods' intermediate precision and robustness a two-step statistical approach was applied. First, Analysis of Variance (ANOVA) was performed to identify significant changes introduced by the applied stress conditions across multiple replicates for each experiment and method ($p<0.05$). Second, to highlight relevant samples showing a significant change in a product attribute, a 95% confidence interval (CI) was specified. This involved comparing stressed samples against their respective control, with the CI set at $\pm$1.96 times the coefficient of variance (CV). For each method, the CV was calculated globally across all replicate measurements of all employed stresses and both serotypes, thereby taking into account run-to-run and serotype-related variability. Importantly, all data with regards to transduction efficiency, capsid titer and FTR were normalized to the results of the control samples obtained by each specific method, as there were considerable differences in absolute readouts using different techniques. Further details on the statistical data assessment, including the sample size, number of replicates, calculated CI and critical F-values (F_{crit}) used for ANOVA are provided in Table S1 in the supplemental information.

Results and discussion

A systematic assessment of a broad panel of analytical methods with regard to their ability to detect stress-induced degradation of AAVs was conducted. For this, two AAV serotypes (rAAV2der and wtAAV9) were subjected to different stress types (i.e. freeze-thaw, thermal, low pH, high pH and light stress). The employed analytical methods were intended to provide a holistic picture on all relevant changes, including their structural integrity, payload stability and the occurrence of post-translational modifications (PTMs), which were correlated with the determined potency of these samples. Statistical evaluation of the results for each method was applied to identify stress-induced alterations that were statistically and practically significant. Their determined experimental CVs alongside other method characteristics are summarized in Table 2. Key observations for each stress condition are described and discussed in the following, and a compilation of all obtained data is provided in the supplemental information (Table S2 -S6).

Impact of freeze-thaw stress on AAV stability

After subjecting rAAV2der and wtAAV9 material to 1, 2, 5 and 10 cycles of freeze-thaw stress, the samples were examined with the standard set of analytical methods.

Most of the samples did not indicate any significant changes in the product attributes assessed, while only a few showed slight trends, mostly within the limits of their determined variability. Specifically, the rAAV2der transduction assay hinted at an initial increase in potency by 18% after the first freeze-thaw cycle compared to the control sample, while this effect reversed after 5 and 10 subsequent cycles. The transient increase in potency can most likely be attributed to method variability, since it showed no uniform trend to higher values and was not backed by any other analytical methods. This is also underlined by the results for wtAAV9, which maintained consistent potency throughout the freeze-thaw stress (Table 1). With regards to size-variants, DLS results revealed a slight reduction of 11% in the hydrodynamic radius (rH) for the size range from 10 to 100 nm (Fig. 1B). Most notably, a significant increase in aggregation of about 3% over the course of 10 freeze-thaw cycles was observed for both serotypes by SEC-UV analysis, accompanied with a decrease in monomer content, while the LMW content remained in a constant range

Table 2
Comparison of analytical methods for characterization of product attributes including precision, throughput, and sample material requirements.

Category	Method	Reported CV [%]	Experimental CV [%]	CI (=1.96 x CV)	Targeted product attribute	Estimated sample throughput/day low (<11), medium, high (>50)	Sample amount per acquisition low (<21μL), medium, high (>100μL)
Statistically evaluated quantitative methods	Potency	5-25[27,28]	3.0	5.9	Transduction efficiency	low	high
	ELISA	10-20[12,26,29]	3.4	6.7	cp titer	high	medium
	Affinity HPLC	-	1.7	3.3	cp/vg titer, FTR	high	low
	SEC-MALS	0-5[17,25,26]	0.6	1.1	cp/vg titer, FTR, aggregation	low	medium
	ddPCR	2-10[18,30,31]	6.1	11.9	vg titer	medium	medium
	MP	0-3[19,32]	1.9	3.7	FTR	medium	low
	Fluorescent DNA staining	<5[33]	0.1	0.2	Free ssDNA	medium	low
	SEC-UV/FLD	<3.5[24]	<0.5	0.6	Aggregation, (free ss/dsDNA)	low	low - medium
	DLS 10-100nm	-	2.6	5.1	Aggregation	medium	medium
	DLS 100-1000nm		29.8 (only for rAAV2der)	58.0			
Not statistically evaluated quantitative methods	PTMS	n.a.	n.a.	n.a.	Post-translational protein modification	low	medium
	NGS	n.a.	n.a.	n.a.	Detailed DNA analysis	low	medium
	CE-SDS	n.a.	n.a.	n.a.	Capsid VP composition	medium	low - medium
Qualitative methods	TEM	n.a.	n.a.	n.a.	Aggregation, capsid integrity, (FTR)	low	Low

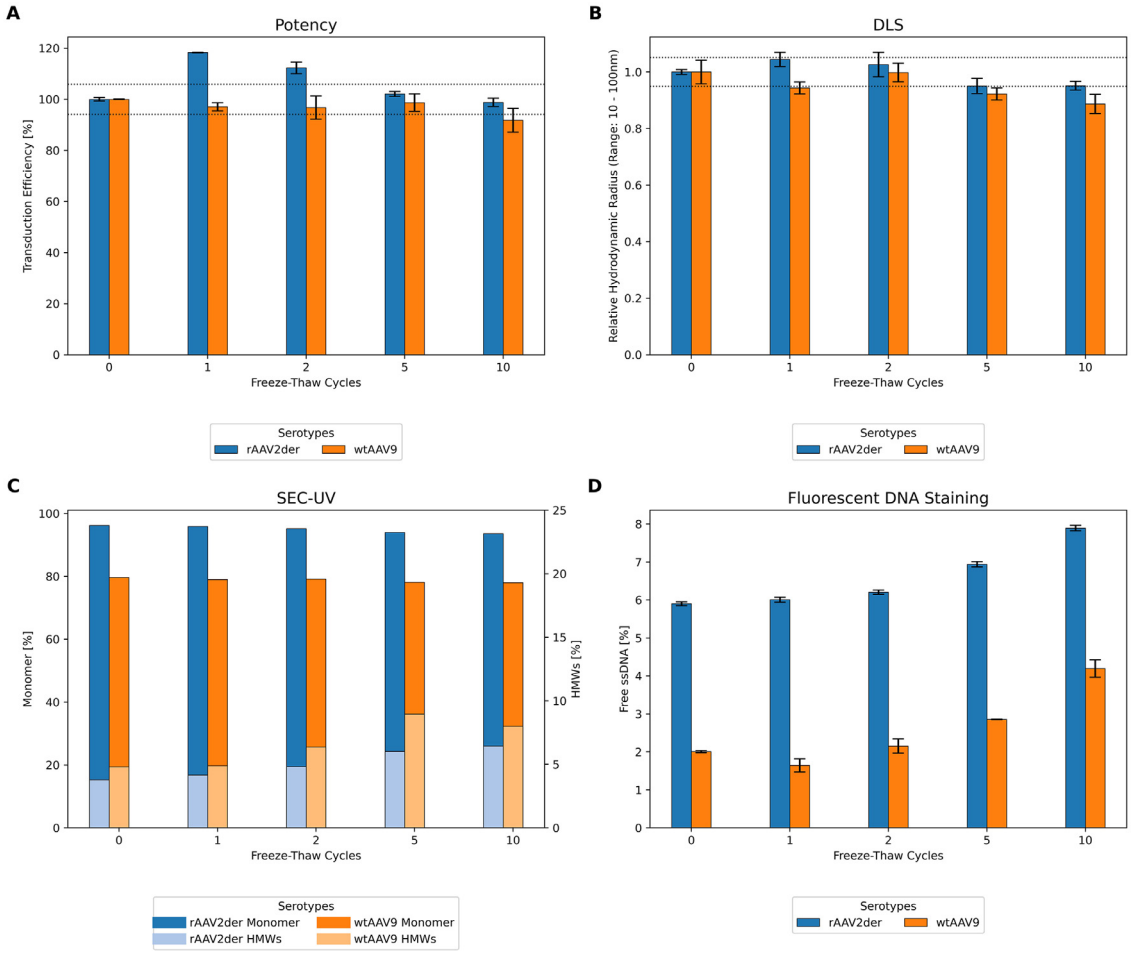

Fig. 1. Results for selected analytical methods after applying freeze-thaw stress: (A) Transduction assay reporting relative potency; (B) Capsid aggregation assessment by dynamic light scattering (DLS) displaying the average hydrodynamic radius in a range from 10 to 100 nm; (C) Relative content of monomer and aggregate content by size exclusion chromatography coupled to UV detection (SEC-UV) (not showing a stable portion of fragments occurring in wtAAV9 samples); (D) Released payload ssDNA in relation to the total payload DNA utilizing a fluorescent ssDNA staining. Results for rAAV2 der are depicted in blue, for wtAAV9 in orange. Scales in (A) and (B) are based on normalization relative to the unstressed control sample (cycle0). The coefficient of variance (CV) for replicate measurements of each sample is indicated by error bars, while the confidence interval (CI) for each method is marked as dotted lines. For better readability, the CI for free ssDNA staining as well as the CV and CI for SEC-UV analysis are not shown.

throughout the F/T study (Fig. 1C). Additionally, the affinity-based HPLC method indicated a gradual loss of capsids up to approximately 5%, which is barely within the method's confidence interval. Finally, we were able to detect an increase in free ssDNA using a Qubit fluorometer by 2% for each serotype throughout the stress study, resulting in relative amounts of 8% free ssDNA for rAAV2der and 4% for wtAAV9, respectively (Fig. 1D).

These findings are generally in good accordance with observations published for serotypes rAAV1, rAAV8 and rAAV9, indicating the release of ssDNA as a result of freeze-thaw stress, as evidenced through a slight increase in the HMW region during SEC-UV analysis and the occurrence of free ssDNA in NGS and fluorimetry. By contrast, the determination of capsid titer and transduction efficiency resulted in no clear trends, which, however, is possibly related to the high coefficients of variation (CVs) of the methods applied in these studies.[5,7,8,28] For the analysis of size variants, the opposite effect was observed: While the results from Wright et al. hinted at an increase of aggregates for both DLS and SE-HPLC analysis[29], a slight reduction of the rH in the size range from 10 to 100 nm was noticeable in our study. These differences may be attributed to the respective AAV serotype and the employed formulation components, such as surfactants, ionic strength and cryoprotectants, which are acknowledged to have a strong influence on AAV capsid stability and aggregational behavior.[5,6,9]

Impact of thermal stress on AAV stability

Samples were subjected to thermal stress at 37°C for a total duration of 14 days, with samples drawn after 2, 4, 8 and 14 days. Subsequent potency analysis revealed a time-dependent, exponential decay of transduction efficiency down to 40 and 20% for wtAAV9 and rAAV2der, respectively (Fig. 2A). As expected, the thermal stress resulted in considerably increased levels of PTMs for both serotypes, especially deamidation at multiple positions. Most notably, rAAV2der was highly susceptible to deamidation at the asparagine residue N57, with an increase up to approximately 50%. By contrast, the deamidation of wtAAV9 at position N57 already plateaued after 4 days of thermal stress at a substantially lower level of ~25%. At site N94, a linear increase in deamidation was observed for both serotypes ultimately reaching values between 20 and 25% after 14 days (Fig. 2B). Further asparagine residues of the AAV capsid proteins were less affected with maximum values in a range between 2 and 3%.

Evaluation of the capsid titer by different analytical methods revealed an overall decrease of intact viral particles, with the largest drop of 15 to 20% for affinity-based HPLC followed by ELISA (~14%) and SEC MALS with values between 4 and 10%. In addition, distinct differences between both serotypes were observed for the FTR, when applying MP and SEC-MALS. Based on MP results, wtAAV9 exhibited a relative decrease of 7% in FTR over time (Fig. 2C), whereas rAAV2der

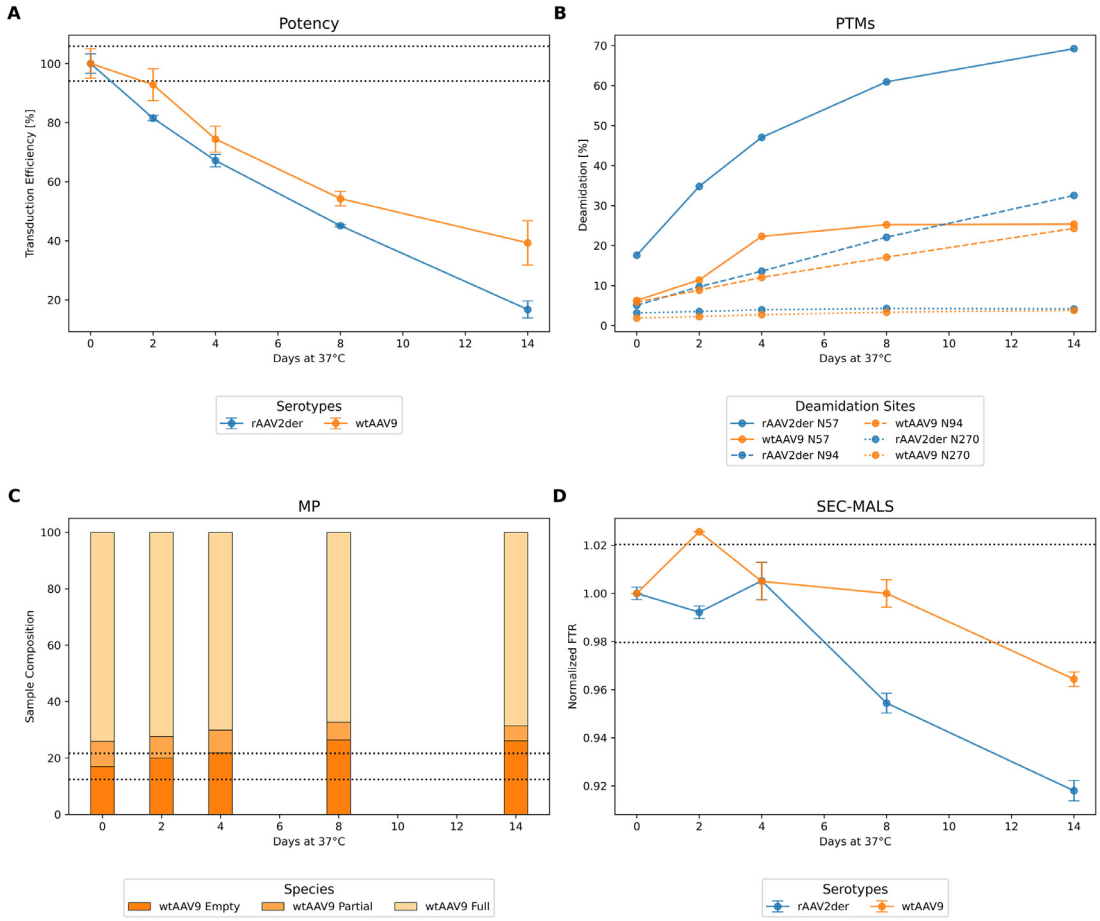

Fig. 2. Results for selected analytical methods after exposure to thermal stress (37°C): (A) Transduction assay reporting relative potency over time; (B)) Estimation of deamidation levels at specific sites (N57, N94, N270) for rAAV2der and wtAAV9 by liquid chromatography coupled to mass spectrometry (LC-MS); (C) Sample composition analysis by mass photometry (MP) indicating the relative proportions of empty, partial, and full capsids for wtAAV9; (D) Normalized full-to-total ratio (FTR) assessed by size exclusion chromatography coupled to multi-angle light scattering (SEC-MALS). Results for rAAV2der are depicted in blue, for wtAAV9 in orange. Relative scales are normalized to the initial time point (day 0). Error bars represent the coefficient of variance (CV) for replicate measurements, while dotted lines indicate confidence intervals (CI). For clarity, CV values are not shown for MP analysis. PTMs were not statistically evaluated.

showed no such effect. Conversely, SEC-MALS indicated a significant decrease in relative FTR of almost 10% for rAAV2der, while only a trend of 4% decrease was found for wtAAV9 (Fig. 2D).

With regards to size variants, SEC-UV revealed a pronounced reduction in oligomers and a concurrent increase in the monomer peak for both serotypes, while SEC-FLD showed no significant changes in fluorescence response. By contrast, DLS demonstrated no evidence of larger-scale aggregation. Fig. 3 provides TEM images of the thermally stressed samples indicating a severe impact of temperature on capsid integrity for both serotypes equally, leading to misshaped and ruptured capsids. Finally, NGS results exposed a slight increase in incomplete, fragmented reads of payload ssDNA (data not shown).

The impact of temperature stress has been investigated in similar experiments using several distinct serotypes, reporting consistent findings with our results; a drastic decrease in potency concomitant with considerably elevated levels of deamidation, but only a small effect on capsid and vector genome titers.[30–32] Of special note is the strong linear correlation between N94 deamidation and the loss of potency in our study (R^2 = 0.992 for rAAV2der and R^2 su 0.969 for wtAAV9; supplemental Fig. S1), as well as the generally high deamidation levels observed at N57. The finding that asparagine deamidation qualifies as a serotype-independent indicator of temperature-induced degradation is in accordance with former studies, confirming its role as potential critical quality attribute (CQA). As previously reported, the associated changes in the surface charge profile could be resolved for rAAV1 and rAAV8 by analytical anion exchange chromatography (AEX) based on the observed peak shifts to the acidic region.[33–35] Although not systematically evaluated in this work for other stress studies, we conducted a choline-buffer based AEX method[36] for rAAV2der to assess if this serotype shows a similar chromatographic behavior. Indeed, while achieving baseline-separation between full and empty capsids for the control sample, full capsids were less retained on the column after temperature stress, resulting in a partial co-elution with empty capsids and therefore altering the readout for the FTR determination.

Impact of high pH stress on AAV stability

The effects of high pH stress (i.e. pH 9.2) on the two serotypes were assessed over a 14-day period, with samples being collected after 2, 4, 8, and 14 days, followed by buffer exchange prior to the analysis. Their transduction efficiency remained largely unaffected throughout the study ranging in between 95 and 108% (Fig. 4A) compared to the unstressed control, which is, at first glance, in conflict with the findings from PTMs, showing a moderate increase in deamidation at position N57 by up to 20%, while other investigated sites did not display any significant increase in comparison to the control sample (Fig. 4B). Deamidation at this site is of specific interest, as N57 is part of the unique sequence of VP1 (VP1u) bearing a phospholipase

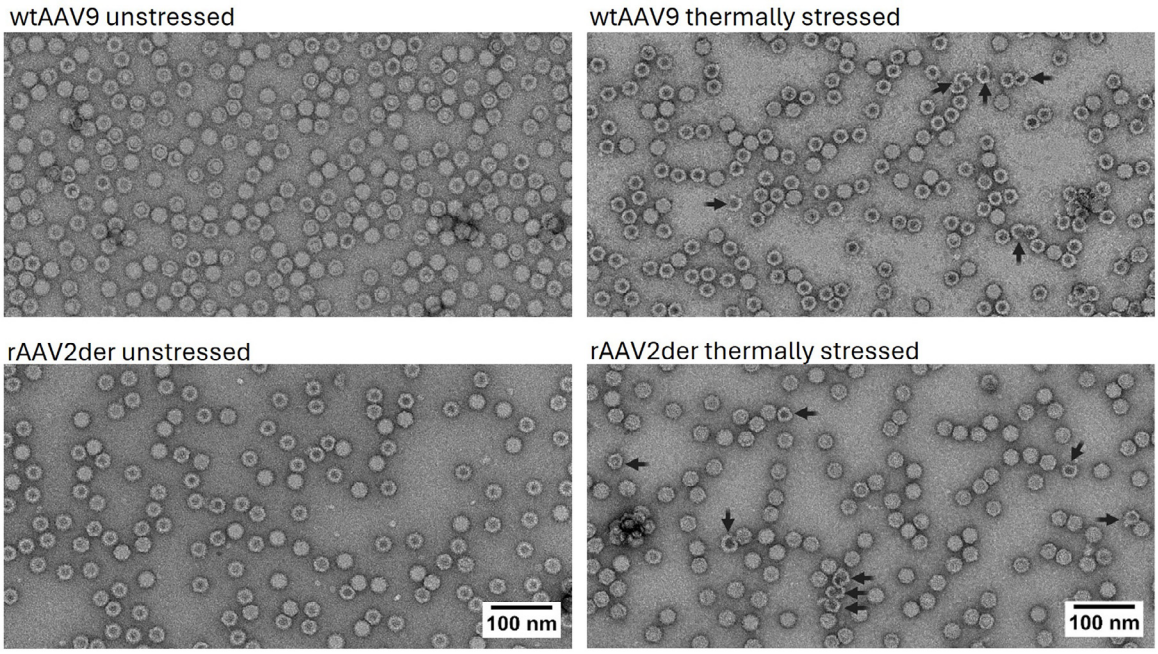

Fig. 3. 50,000x magnified negative-stain transmission electron microscopy (TEM) images of wtAAV9 (top) and rAAV2der (bottom) to detect non-intact and misshaped capsids (exemplarily marked with arrows; right) after thermal stress at 37°C for two weeks in comparison to non-stressed controls (left).

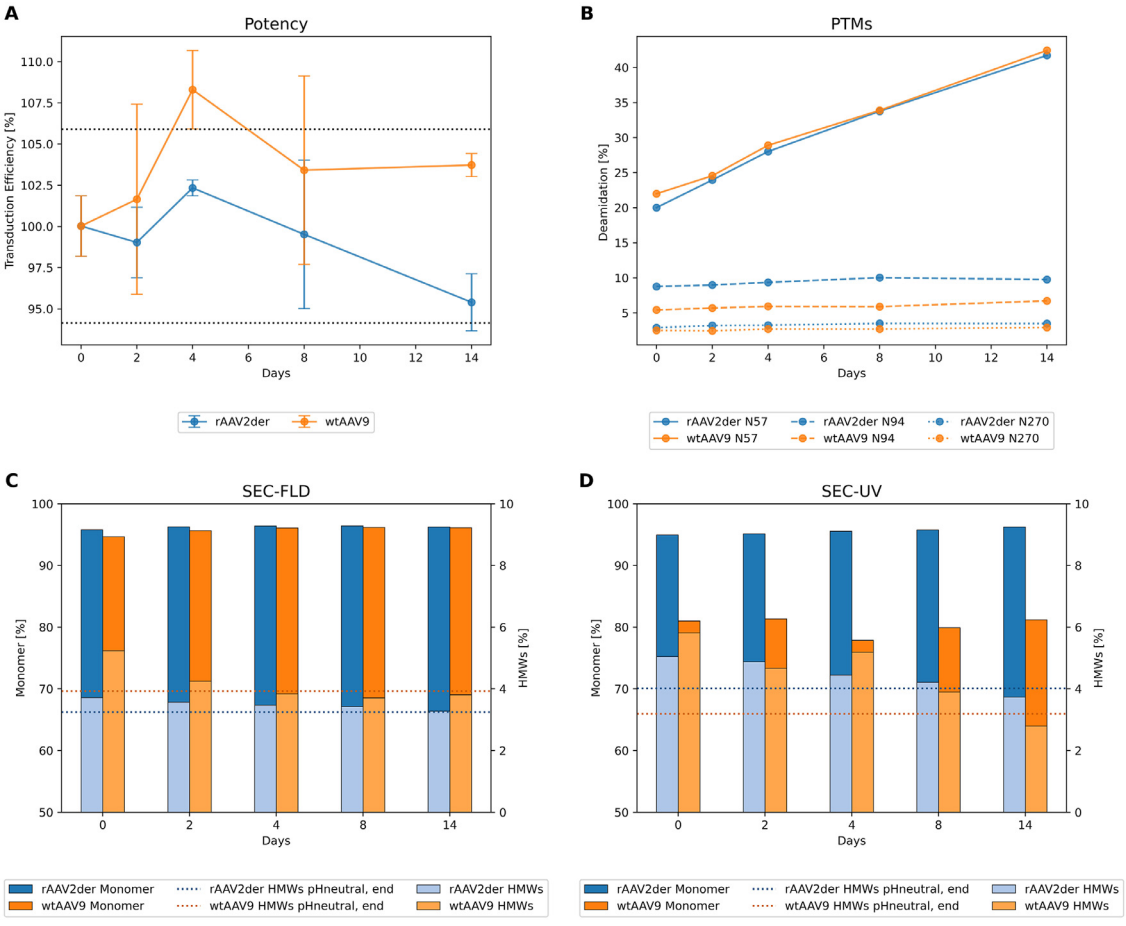

Fig. 4. Analysis of rAAV stability under high pH (9.2) conditions at 4°C using selected analytical methods: (A) Transduction assay reporting relative potency over time; (B) Estimation of deamidation levels at specific sites (N57, N94, N270) for rAAV2der and wtAAV9 by liquid chromatography coupled to mass spectrometry (LC-MS); (C) Relative monomer and high molecular weight species (HMWS) content analyzed by size exclusion chromatography coupled to fluorescence detection (SEC-FLD); (D) Monomer and HMWS content assessed by size exclusion chromatography coupled to UV detection (SEC-UV). Results for rAAV2der are depicted in blue, for wtAAV9 in orange. Colored dotted lines in (C) and (D) indicate the endpoint of HMWs in the control sample at neutral pH for the respective serotype. Relative scales are normalized to the initial time point (day 0). In (A), error bars represent the coefficient of variance (CV) for replicate measurements, while dotted lines indicate confidence intervals (CI). CV and CI are not shown for SEC analysis. Post-translational modifications (PTMs) were not statistically evaluated.

A2 (PLA2)-like motif that is linked to endosomal/lysosomal escape of AAVs capsids during endocytosis.[37,38] Previous studies regard this PTM as a potential CQA, indicating loss in transfection efficiency.[39,40] By applying a lower temperature of 4°C during pH stress, our approach aimed at isolating the effect of pH stress from that of temperature-induced deamidation (or potential synergistic effects). In this regard, the finding that the sole deamidation of N57 showed no significant impact on potency, suggests the assumption that the observed loss in transduction efficiency after thermal stress is a result of the combination of several alterations on capsid and payload level. However, additional investigation of other rAAV serotypes is required to allow general applicability of our findings and to advance the identification of potential CQAs of rAAVs with regards to PTMs.

Determination of genome and capsid titer yielded some interesting insights. Whereas the overall alterations were rather small and mostly within the confidence intervals of the applied methods, MP analysis exhibited for rAAV2der an increase in empty capsids by roughly 6%, thereby lowering the FTR. Additionally, SEC-MALS analysis of wtAAV9 hinted at an increase in capsid titer over the course of the experiment, which however could also be observed in the control sample. A potential cause for this counterintuitive behavior can be derived from structural assessment using SEC-FLD and SEC-UV. Both methods pointed to a shift toward higher monomer and lower HMWs content with increased stress time, which was also observed for the respective control samples that were incubated at standard formulation conditions (Fig. 4C and D). Consequently, the observed disaggregation of HMWs is likely rather an artifact of the initial stock preparation than an effect of the high pH conditions applied. As the performed buffer exchange led to a temporary increase in capsid concentration on the order of E15 cp/mL, we assume that this step has induced the formation of reversible oligomeric aggregates.[41] These HMW variants dissociated again to the monomeric forms within 4 days after dilution to the target concentration range of 1E14 cp/mL. By contrast, DLS results suggest an increase of larger, probably irreversible aggregates within the 100-1000 nm size range for rAAV2der over the incubation time at elevated pH. While these results indicate an additional aggregational behavior of rAAV2der, further investigation of this effect is required due to the high variability of the DLS method in this size range and the potential impairment introduced by reversible aggregation via the concentration step.

Impact of low pH stress on AAV stability

Prior to selecting the conditions for low pH stress we performed an extensive literature review to identify potential gaps. Most studies were performed at pH 4-6, representing the physiological conditions during endosomal trafficking following the uptake of capsids into cells. Structural X-Ray analysis of rAAV8 capsids within this pH range suggests that reversible conformational changes in the N-terminal region of the unique sequence of VP1 (VP1u) potentially lead to an externalization of the PLA2-like domain.[42,43] In addition, a potency loss was previously reported at pH 5-6 for rAAV9, coinciding with increased thermostability of capsids.[44] Although DNA-protein interaction should be reduced at low pH, the authors observed no genome ejection. Furthermore, it was shown for several serotypes that the pH range causing changes in thermostability and transduction efficiency is serotype-specific and the effects are temperature dependent. While frozen or cooled samples at 4°C largely exhibited capsid stability down to pH 4, samples kept at RT or elevated temperature of 37°C and a pH of 2.5 displayed a drastic decrease in potency.[10,30] Based on these findings, we were especially interested in further investigating the pH range between 2.5 and 4.0, which often is utilized as elution condition for affinity purification during downstream processing. Additionally, we targeted for a lowered temperature of 4°C to exclude any temperature-induced effects and further extend the insights into rAAV stability in the acidic pH range.

Low pH stress (pH 3.0) on the two investigated rAAV serotypes, rAAV2der and wtAAV9, yielded contrasting outcomes. Transduction efficiency for rAAV2der increased to approximately 140% after applying low pH stress for 14 days, while wtAAV9 exhibited a drop down to approximately 75%, both showing a consistent linear trend over the course of the stress (Fig. 5A). Determination of capsid titer and vector genome titer for rAAV2der resulted in mixed results, with a reduction of capsid titer of approximately 8% according to Affinity HPLC data and at the same time a vg titer increase of nearly 20% as per ddPCR results (Fig. 5B and C). The latter finding negates the assumption that changes in vector genome titer are solely responsible for the observed increase in potency, suggesting that additional product attributes (e.g., purity, capsid integrity and alteration, aggregation) have an impact on the read-out of the applied transduction assay. For wtAAV9, a slight increase in capsid titer of approximately 5% was observed for both stressed and unstressed samples using SEC-MALS, consistent with the observations under high pH stress. By contrast, neither Affinity HPLC nor ddPCR gave a hint towards the loss of capsids or vector genomes for wtAAV9, which could explain the loss in transduction efficiency.

In accordance with the results for high pH stress, disaggregation of wtAAV9 oligomers was apparent under low pH conditions. This was evidenced by SEC-UV results, showing a reduction in HMW forms after 14 days from 6% to 2% and 3% for the stressed (low pH) and the unstressed (control) samples, respectively. Similarly, SEC-FLD data suggested a comparable trend, reducing the level of HMWs from 5,5% to 4% for both stressed and unstressed samples. By contrast, rAAV2der exhibited only minimal changes in size variant profiles, with the emergence of a fragment peak in SEC-UV representing up to 2% of the total peak area, indicating free, non-aggregated DNA as the most noticeable alteration (Fig. 5D). While the relation of these free DNA fragments on the observed increase in vg titer and transduction efficiency remains elusive based on the present data, we speculate that this behavior could point towards a serotype-specific disaggregation of larger HMW forms resulting in the demasking of potent capsids.[29] As a result of the demasking, the accessibility of potent capsids carrying the DNA payload during capsid digest would be improved, leading to a higher functional vg titer as detected by PCR.

Impact of light stress on AAV stability

The impact of light exposure on capsid and payload integrity was assessed for rAAV2der and wtAAV9 under either mild light stress conditions (i.e. filtered UV) for 50 h or harsh UV stress for 24 h, fulfilling the requirements for Option 1 D65 light sources according to ICH Q1B.[45] Under mild stress, a slight reduction of the transduction efficiency of approximately 10% was observed, which however did not translate to any meaningful changes for the entire panel of applied analytical methods. Therefore, the results presented below focus on the effects of UV light exposure.

Bioactivity experiments indicated an almost complete loss of transduction efficiency following UV stress for both serotypes relative to the dark control (Fig. 6A). Capsid titers determined by ELISA (Fig. 6B) and Affinity HPLC hinted at a decrease by 8 to 13% for both serotypes. By contrast, SEC-MALS analysis was unable to resolve any significant changes for rAAV2der but suggested a ~20% increase in capsid titer for wtAAV9, while the obtained FTR decreased by 10%.

With regards to size variants, SEC-FLD indicated an increase in oligomers for both serotypes by 2.5%, suggesting moderate capsid aggregation which can serve as potential explanation for the aforementioned loss in capsid titer. Using SEC-UV, no noticeable change was obtained for rAAV2der, while wtAAV9 exhibited a loss of LMWs.

Payload analysis of rAAV2der applying NGS demonstrated pronounced ssDNA fragmentation with a broad density distribution of read lengths between 1 and 3500 bp and a maximum at ~1000 bp.

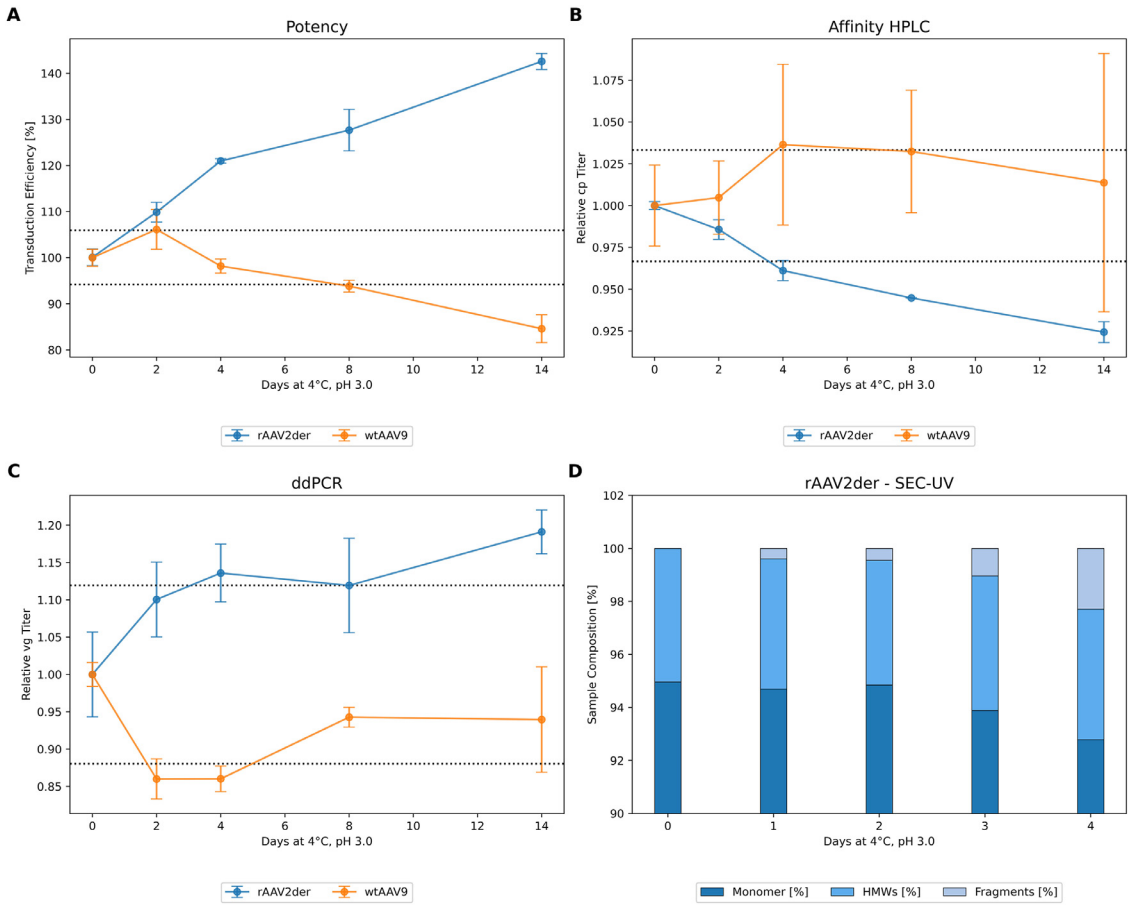

Fig. 5. Evaluation of rAAV stability under low pH (3.0) conditions at 4°C by selected analytical methods: (A) Transduction assay reporting relative potency over time; (B) Size exclusion chromatography coupled to UV detection (SEC-UV), analyzing the relative proportions of monomers, high molecular weight species (HMWS), and fragments for rAAV2der; (C) Relative vector genome (vg) titer determined by droplet digital PCR (ddPCR); (D) Capsid titer (cp) assessed by affinity HPLC. Results for rAAV2der are depicted in blue, for wtAAV9 in orange. Scales are normalized to the initial time point (day 0). Error bars represent the CV for replicate measurements, while dotted lines indicate the methods' CI. CV and CI values are not shown for SEC-UV analysis.

For wtAAV9, a similar yet less severe fragmentation behavior was observed, as evidenced by the peak at ~4000bp suggesting a remaining population of intact payload DNA (Fig. 6C). Additionally, the number of total reads decreased by 75% for rAAV2der up to 90% for wtAAV9. While ddPCR displayed a non-significant loss of about 10% vg for both serotypes, further characterization of the observed ssDNA fragmentation of the samples by capillary electrophoresis using the 5300 Fragment Analyzer System (Agilent) provided no indication of fragmentation of the ssDNA backbone (data not shown).

Strong oxidation of the capsid was observed at position M203 and less pronounced but significant at M434 and M436 for rAAV2der and wtAAV9, respectively. When analyzing the capsid proteins by CE-SDS, the UV light exposed samples exhibited a marked change in VP-ratio with decreased portions of VP1 and VP2 (Fig. 6D). Furthermore, an additional high molecular weight species emerged which was not noticeable for any other stress conditions. Fluorimetry analysis revealed a slight increase of free ssDNA in a range of 0.8 and 1.7% relative to total ssDNA. More interestingly, performing the same analysis after enforced thermal ejection resulted in a considerable decrease in the detectable amount of ssDNA compared to the control samples, which might be attributed to an incomplete release of ssDNA due to DNA-protein crosslinking. Consequently, our findings indicate severe effects on both the DNA and capsid level, possibly compromising the dsDNA synthesis and the repair step during NGS library preparation, hence leading to unsuccessful reads of full-length payload DNA while overestimating smaller DNA fragments.

To our knowledge, the understanding of light-induced stress on the stability of rAAVs is still limited. Takino et al applied UV light induced stress on rAAVs, resulting in similar observations. Besides an increasing amount of atypical HMWs by Capillary Gel Electrophoresis (CGE), the investigated rAAV6 capsid displayed increased oxidation of M372 and M403. In addition, the formation of cyclobutane pyrimidin dimers (CPD) was observed, which reportedly affects the conformational integrity of ssDNA.[40] It is noteworthy that - in contrast to the findings of this study - we only detected an insignificant decrease in genomic titer when applying ddPCR. The apparent increase in capsid titer for wtAAV9 via SEC-MALS is likely caused by changes in the physicochemical properties of the stressed samples. We hypothesize that the severe impact of UV stress, which did not only affect the DNA payload but also the capsid integrity, resulted in a deviating detection behavior that interferes with accurate determination of the capsid titer by SEC-MALS. In this regard, the effect of light-induced crosslinks, either on protein-protein or protein-DNA level, as well as alterations of the payload sequence by depurination or dimerization, should be assessed in future studies regarding potential implications on the reliability of the employed analytical methods.

Systematic comparison of analytical methods applied throughout different stresses

During this study, the standard set of analytical methods, covering payload titer, size variant composition and transduction efficiency,

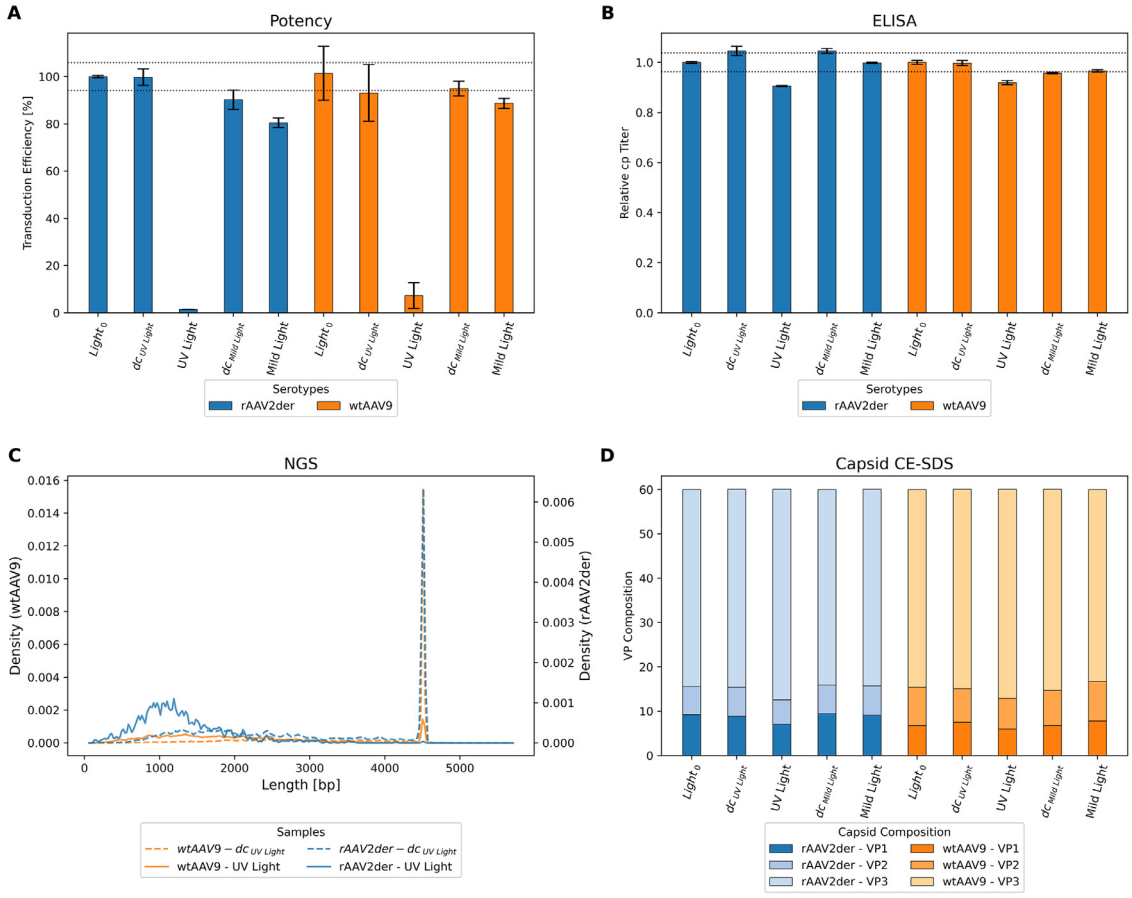

Fig. 6. Assessment of rAAV stability under UV or mild light exposure by selected analytical methods: (A) Transduction assay reporting relative potency; (B) Capsid titer determined by ELISA, normalized to the untreated control (Light0); (C) Genome integrity analysis by next-generation sequencing (NGS), showing the distribution of genome lengths for rAAV2der and wtAAV9. Solid lines represent UV-stressed samples, while dotted lines indicate unstressed controls; (D) Capsid protein composition analyzed by CE-SDS, displaying the proportions of VP1, VP2, and VP3. Results for rAAV2der are depicted in blue, for wtAAV9 in orange. Error bars represent the CV for replicate measurements, while dotted lines indicate the respective CI. For clarity, CV and CI values are not shown in (D). NGS was not statistically evaluated.

was evaluated statistically applying a one-way ANOVA. Significant changes in samples after stress application were identified relative to unstressed controls, considering the coefficient of variation (CV) for each method (shown in Table 2). This allowed a comparison of the significance of the results, also with regard to previously published findings. Despite this statistical approach to identify relevant stress-induced sample alteration, it cannot be entirely excluded that single samples show outlying behavior. To account for this, only observations were deemed meaningful that occurred across multiple sampling points or showed an overall trend to higher or lower values. In general, results demonstrated good agreement with the available data for different stress conditions. Highly automated methods, involving only limited manual preparation steps such as SEC-UV/FLD, Affinity HPLC and MP, achieved high accuracy with CVs below 2%. By contrast, analytical methods depending on multiple sample processing steps, including the preparation of serial dilutions, as performed for AAV ELISA, often showed increased CVs. Most severely, enzymatic or cell-based assays resulted in the highest CVs ranging from 3.9% for potency to 6.1% for ddPCR, which can be explained by the inherent biological variability and complexity of these assays.

In line with established practices for *in vitro* potency assessment of rAAVs, we employed a serial-dilution transduction assay in HEK293 cells with a GFP expression readout by flow cytometry. Samples were evaluated by fitting the dose-response and comparing the quasi-linear range relative to the respective non-stressed control samples. Comparable transduction assays have been reported applying different analytical read-outs, such as imaging of fluorescent reporters, immunocytochemistry with chromogenic detection, enzymatic activity, and flow cytometric quantification of reporter-positive cells.[8,10,27,28,31,32,46] In contrast to single-point transduction designs at fixed MOI (i.e. single dose response experiments) that are frequently applied as simplified versions, our assay design provides high reliability for determining the relative transduction, which is considered essential when product attributes vary significantly between samples due to stress exposure.[7,8,10,32,40] Given the inherent biological complexity of transduction depending on multiple factors such as rAAV uptake, cell state heterogeneity, second-strand synthesis, promoter activity and reporter maturation kinetics, the herein conducted assay merely reflects the functional endpoint and is hence less suited for pinpointing the structural or biochemical changes to a specific cellular process. For deeper mechanistic attribution, additional assays that explicitly resolve entry, trafficking, genome delivery, and payload function are recommended. This for example includes two-color co-transduction by FACS to estimate co-delivery and multi-hit probabilities consistent with Poisson loading, single-cell ddPCR or viral barcoding to directly count vector genomes per cell, and PCR of intracellular or nuclear genomes to resolve entry and trafficking steps upstream of reporter expression.[37]

For the evaluation of size variants, the capsid titer and the vector genome, a broad panel of well-established analytical techniques was employed in parallel for the different stress conditions. Utilizing this extensive dataset allowed us to draw conclusions on the capabilities of these methods to indicate stress-related alterations for the AAV serotypes investigated. SEC coupled with UV or fluorescence

detection is the method of choice for evaluating LMW and HMW (including capsid dimers and oligomers) forms of AAVs. Combining these two detection modes proved especially helpful to resolve changes both on protein and DNA level. While SEC-FLD is aptly suited to monitor the formation of (small) aggregates and capsid fragments, the UV signal, relying on the A260/A280 ratio, can be exploited to derive additional information on the DNA content of the obtained species. In our study, SEC-UV analysis of thermally stressed samples indicated a decrease of HMW species, while the proportion of the monomer increased with longer stress time. By contrast, the relative peak areas remained largely unchanged in the FLD traces, suggesting an aggregation behavior at the DNA level. In addition, LMWs fractions detected during low pH stress for rAAV2der in SEC-UV could be attributed to DNA fragments, further highlighting the method's ability to discriminate between protein- and DNA-caused degradation. For the detection of higher-level aggregation, DLS is the most common technique used, particularly in the range between 100 and 1000 nm. Under basic pH as well as elevated temperature stress, DLS results suggested a change in these aggregates, which however was obscured by the high CV of this method. Overall, a relatively high stability against capsid aggregation was observed for the chosen formulation throughout this study, despite the deliberate omission of sucrose as stabilizing agent.

Enzyme-linked immunosorbent assays (ELISAs) are a widely used technique for capsid determination of AAVs.[12,13,47] This is because of its high throughput and the ability to analyze samples throughout the entire bioprocess with low material requirements. However, commercially available antibodies against AAVs bind reportedly also to non-intact, fragmented or aggregated capsid proteins, potentially leading to titer overestimation.[48] Likewise, our recently introduced Affinity HPLC method exploits the specific binding of the capsid proteins on immobilized AAV antibodies enabling the determination of the capsid titer in the eluting peak. Conceptualized as Process Analytical Technology (PAT) tool, this method allows for fast turnaround times of less than 2 min/sample, which proves especially helpful for processing a high number of samples or can even be directly coupled to the process for online analytics.[14,15,49] On the downside, this method is also reliant on the availability of suitable antibodies against the serotype of interest, might require method optimization for effective binding and elution of the rAAVs, and initial calibration using orthogonal analytics is required. Besides these techniques relying on AAV antibodies, SEC-MALS was applied as a third method to determine the capsid titer after different stresses. Since the MALS detection of the AAVs is preceded by chromatographic separation of HMWs and LMWs, the effective titer of the desired AAV monomer should in theory be determined more reliably than for AAV ELISA and Affinity HPLC. Interestingly, antibody-based methods exhibited during our study a higher sensitivity to detect stress-induced alterations in the rAAV samples investigated, as can be concluded from the increased loss of capsids during temperature and UV light stress. In addition, the Affinity HPLC was also capable of hinting at a slight loss of capsids during freeze-thaw stress. We suggest that the higher capacities of AAV ELISA and, particularly, Affinity HPLC to report degradation inflicted by stress conditions is due to their susceptibility to (local) surface changes affecting the interaction of the AAV with the employed antibodies. By contrast, SEC-MALS can only resolve the overall integrity of rAAV capsids and is consequently insensitive to subtle changes in surface topology that do not significantly alter the capsids' hydrodynamic radius.

In addition to determining the capsid titer, SEC-MALS has emerged as a powerful tool for calculating the FTR based on the molecular properties of the capsid. A key advantage is that the analysis can be performed in a single, calibration-free measurement.[17,18,50] However, data interpretation can be challenging due to the heterogeneous nature of AAV samples. This complexity, combined with typical run times of 20 to 40 minutes, makes the technique less suitable for high-throughput applications, as for example required during process development. Due to these limitations, the combination of capsid titer determination by ELISA and vector genome quantification by (dd)PCR is commonly applied as an alternative approach for obtaining the FTR. On the downside, this two-method solution is inherently prone to error. Both individual assays already exhibit considerable methodological variability. By combining them, their respective coefficients of variation (CVs) are compounded, which significantly increases the potential for inaccuracy in the final FTR result. In addition, our employed ddPCR setup was not able to detect the degradation of the DNA payload after UV light stress, which resulted in complete loss of transduction efficiency and severe DNA fragmentation as evidenced by NGS. This highlights the importance of properly designing the primers/probes and their position to reliably detect truncated or fragmented genomes.[51]

Overall, the currently prevailing absence of comprehensive analytical methods to reliably detect changes in product attributes of rAAVs, mandates a combined approach covering a broad panel of different techniques for early method and process development. Only through such a strategy, can a reasonable understanding of the product and the associated process be achieved.

In this study, we applied this approach to identify the most appropriate analytical method for a given product attribute and stress condition as well as revealing potential inconsistencies between orthogonal techniques. The key findings of this study are shown in Table 3, summarizing the most sensitive methods for detecting changes in relevant product attributes according to the stress factor investigated. The use of orthogonal methods proved critical to reliably detect stress-induced alterations that might otherwise be insufficiently recognized or entirely overlooked by employing a single assay, thereby taking into account the different assay principles.

For instance, we observed that capsid titer alterations in some stressed samples were more pronounced when applying affinity-based methods (e.g., ELISA or Affinity LC). By contrast, SEC-MALS, despite its higher accuracy and lower CV, turned out to be less sensitive in these cases. This discrepancy suggests that the observed changes were primarily triggered by the level of interactions between the rAAV and the employed antibodies rather than structural changes at the capsid level. Similarly, determination of FTR utilizing SEC-MALS, ELISA/ddPCR and MP varied considerably for the investigated samples. Particularly under thermal stress conditions, SEC-MALS and MP provided ambiguous readouts, rendering interpretation challenging due to the lack of confirmatory data from a well-characterized method. This example, along with other observations made throughout this study, underscores the need for focusing on the development of stability-indicating methods as part of a robust analytical control strategy. For this, established analytical workflows need to be carefully evaluated regarding their technical limitations, especially for new capsid-payload combinations and after adapting the process conditions.

Insights into rAAV sample handling

During this study, sample handling proved critical for ensuring reliability of the obtained analytical results. For example, pre-experiments showed that freeze-thawing steps can result in marked sample heterogeneity, which in turn can significantly affect the assessment of capsid titer and other product attributes. In this regard, the formation of concentrated patches following freeze-thaw stress led to sample heterogeneity and subsequent capsid titer variations of up to 20% (data not shown). To mitigate this effect for the samples evaluated throughout this study, short vortexing (<5s) proved practical to ensure homogeneity without inducing artifacts, such as aggregates. It is important to note that the impact of vortexing on sample stability was only assessed for the serotypes investigated throughout this study and that these findings cannot necessarily translated to other

Table 3
Summary of the key responses of analytical methods.

Stress factor (Detailed table in supplement)	Quality attribute	Lead method	rAAV2der	wtAAV9
Freeze-Thaw (Table S2)	Capsid titer	Affinity HPLC	-5.0 %	-5.0 %
	Aggregation	SEC-UV	+2.7 % HMWs	+3.2 % HMWs
	Genome release	ssDNA staining	+2.0 %	+2.2 %
	Hydrodynamic-Radius (10-100 nm)	DLS	No significant change	-11 %
Thermal (37°C) (Table S3)	Potency	Bioassay	-83 %	-60 %
	Deamidation	PTMs by LC-MS	+50 % (N57), +25 % (N94)	+25 % (N57), +20 % (N94)
	FTR	SEC-MALS/MP	-8.0 % (SEC-MALS)	-7.0 % (MP)
	Capsid titer	Affinity HPLC	-15.0 %	-20.0%
High pH (9.2) (Table S4)	Deamidation	PTMs by LC-MS	+20 % (N57)	+20 % (N57)
	FTR	MP	-15 % (+6 % empty capsids)	No significant change
	Hydrodynamic radius (100-1000 nm)	DLS	+ 76 %	No significant change
Low pH (3.0) (Table S5)	Potency	Bioassay	+43 %	-15 %
	Capsid titer	Affinity HPLC	-9 %	No significant change
	Genome titer	ddPCR	+20 %	No significant change
	Impurities	SEC-UV	+2 % fragments	No significant change
UV Light (Table S6)	Potency	Bioassay	-98 %	-93 %
	Payload integrity	NGS	Completely fragmented; ~75 % of total reads	Massive fragmentation; ~90 % of total reads
	Genome release	ssDNA staining	+0.8 %	+1.7 %
	Capsid titer	Affinity HPLC/ (ELISA)	-13 % (-9 %)	-8 % (-8 %)
	Aggregation	SEC-FLD	+2.6 %	+2.4 %

serotypes. For larger volumes (>10 mL), we recommend extensive sample rolling. Short-term storage (up to three weeks) of rAAV samples at neutral pH and 4°C had no impact on sample homogeneity and titer stability, although slight molecular changes, including increased deamidation levels, were observed, which should be considered for subsequent analyses.

For performing pH stresses, centrifugal concentration using ultra centrifugal filters was effective for buffer exchange of formulated rAAV samples and yielded a recovery between 95-100%. On the downside, the herein applied protocol resulted due to a strong concentration effect of the AAV samples during the filtration process in the formation of aggregates. While these aggregates proved to be largely reversible within a timeframe of a few days and did not impair the overall capsid stability, this effect interfered with reliable HMW analysis by SEC for high/low pH stress. This finding emphasizes the need for standardized handling protocols to eliminate confounding factors affecting consistent analytical outcomes.

Conclusion

Two distinct rAAV serotypes were exposed to different stresses and analyzed by applying a broad range of common analytical tools to investigate both the sensitivity of methods towards stress related sample alteration as well as the influence of the applied stress on capsids and payload. Results from transduction efficiency testing displayed considerable differences of stress response indicating almost complete attrition of rAAVs through harsh UV light stress and exposure to elevated temperatures, whereas no significant changes for high pH, freeze-thaw cycles and mild light stress were observed and in parts even an increase of potency after low pH exposure.

Except for the UV light stress, where the reduction of transduction efficiency correlated with the fragmentation of the payload as determined by NGS, for other kinds of stresses no clear correlation could be established, suggesting a complex interplay between different product attributes that cannot be resolved by existing analytical methods. The investigation of root causes leading to changes in potency was furthermore restricted by technical limitations of these assays stemming from low analyte titers in combination with an inherently higher complexity compared to other therapeutic modalities. In addition, our findings indicate considerable differences in AAV behavior upon stress conditions depending on the employed rAAV serotype, underlining the necessity of serotype-specific development of analytical control strategies.

Overall, the outcome of our study signifies a strong need for developing stability-indicating analytical methods tailored for quality control and characterization of rAAV-based gene therapies to ensure consistent quality and streamline their development.

Funding

This research did not receive any specific grant from funding agencies in the public, commercial, or not-for-profit sectors.

Declaration of generative AI in scientific writing

During the preparation of this work the authors used an in-house AI-companion application (based on the GPT3.5 turbo 16k version of Azure OpenAI) in order to rephrase some passages and for grammar check. After using this application, the authors reviewed and edited the content as needed and take full responsibility for the content of the publication.

CRediT authorship contribution statement

Jakob Heckel: Writing – original draft, review and editing, Visualization, Methodology, Investigation, Conceptualization, Data

Curation, Formal Analysis. **Lukas Bongers:** Writing - original draft, review and editing. **David Naylor:** Investigation, Methodology. **Ole Schmidt:** Investigation, Data Curation. **Raphael Ruppert:** Resources, Conceptualization. **Marco Thomann:** Conceptualization, Writing – review and editing. **Florian Semmelmann:** Writing – review and editing **Angie Kirchner:** Investigation, Writing – review and editing. **Alexandra H.E. Machado:** Conceptualization, Writing – review and editing. **Markus Haindl:** Resources, Funding Acquisition, Project Administration. **Michael Leiss:** Supervision, Conceptualization. **Jürgen Hubbuch:** Supervision, Conceptualization, Writing – review and editing. **Tobias Graf:** Writing – original draft, review and editing, Formal Analysis, Visualization.

Data availability statement

Roche Diagnostics GmbH is unable to provide materials, additional datasets, or protocols.

Declaration of competing interest

All authors, except for Jürgen Hubbuch, are current employees of Roche Diagnostics GmbH and some authors declare stock ownership in the Roche Holding AG.

Acknowledgements

The authors would like to express their gratitude to our colleagues from the analytical departments and formulation development teams within PTCG, PTDA, PTDP, and pRED for their valuable contributions and support.

We are particularly grateful to Irini Skaripa-Koukelli, Johannes Pschirer, Christoph Gstöttner, Roberto Falkenstein, Andrés Martinez, Timo Bohlig, Julia Manz, and Alina Fuhrmann for insightful discussions and their input, which greatly enriched this work.

Supplementary materials

Supplementary material associated with this article can be found in the online version at doi:10.1016/j.xphs.2026.104257.

References

1. Zwi-Dantsis L, Mohamed S, Massaro G, Moeendarbary E. Adeno-associated virus vectors: principles, practices, and prospects in gene therapy. *Viruses*. 2025;17(2):239. https://doi.org/10.3390/v17020239.
2. Wörner TP, Bennett A, Habka S, et al. Adeno-associated virus capsid assembly is divergent and stochastic. *Nat Commun*. 2021;12(1):1642. https://doi.org/10.1038/s41467-021-21935-5.
3. Shmidt AA, Egorova TV. PCR-based analytical methods for quantification and quality control of recombinant adeno-associated viral vector preparations. *Pharmaceuticals*. 2021;15(1):23. https://doi.org/10.3390/ph15010023.
4. Srivastava A, Mallela KMG, Deorkar N, Brophy G. Manufacturing challenges and rational formulation development for AAV viral vectors. *J Pharm Sci*. 2021;110(7):2609–2624. https://doi.org/10.1016/j.xphs.2021.03.024.
5. Xu Y, Jiang B, Samai P, Tank SM, Shameem M, Liu D. Genome DNA leakage of Adeno −Associated virus under freeze−thaw stress. *Int J Pharm*. 2022;615:121464. https://doi.org/10.1016/j.ijpharm.2022.121464.
6. Bee JS, Zhang Y, Finkner S, et al. Mechanistic studies and formulation mitigations of adeno-associated virus capsid rupture during freezing and thawing mechanisms of freeze/thaw induced AAV rupture. *J Pharm Sci*. 2022;111(7):1868–1878. https://doi.org/10.1016/j.xphs.2022.03.018.
7. Chan A, Maturana CJ, Engel EA. Optimized formulation buffer preserves adeno-associated virus-9 infectivity after 4°C storage and freeze/thawing cycling. *J Virol Methods*. 2022;309:114598. https://doi.org/10.1016/j.jviromet.2022.114598.
8. Howard DB, Harvey BK. Assaying the stability and inactivation of AAV serotype 1 vectors. *Hum Gene Ther Methods*. 2017;28(1):39–48. https://doi.org/10.1089/hgtb.2016.180.
9. Motabar L, Palakollu V, Shahfar H, et al. Impact of electrostatics on the aggregation, genome release, and self-interactions of AAV9 capsids. *J Pharm Sci*. 2025;114(9):103899. https://doi.org/10.1016/j.xphs.2025.103899.
10. Lins-Austin B, Patel S, Mietzsch M, et al. Adeno-Associated Virus (AAV) capsid stability and liposome remodeling during endo/lysosomal pH trafficking. *Viruses*. 2020;12(6):668. https://doi.org/10.3390/v12060668.
11. Gupta V, Lourenço SP, Hidalgo IJ. Development of gene therapy vectors: remaining challenges. *J Pharm Sci*. 2021;110(5):1915–1920. https://doi.org/10.1016/j.xphs.2020.11.035.
12. Cui M, Lu Y, Tang C, et al. A generic method for fast and sensitive detection of adeno-associated viruses using modified AAV receptor recombinant proteins. *Molecules*. 2019;24(21):3973. https://doi.org/10.3390/molecules24213973.
13. Grimm D, Kern A, Pawlita M, Ferrari FK, Samulski RJ, Kleinschmidt JA. Titration of AAV-2 particles via a novel capsid ELISA: packaging of genomes can limit production of recombinant AAV-2. *Gene Ther*. 1999;6(7):1322–1330. https://doi.org/10.1038/sj.gt.3300946.
14. Heckel J, Martinez A, Elger C, et al. Fast HPLC-based affinity method to determine capsid titer and full/empty ratio of adeno-associated viral vectors. Mol Ther - Methods Clin Dev. 2023;31:101148. https://doi.org/10.1016/j.omtm.2023.101148.
15. Heckel J, Bohlig T, Bonnington L, et al. Rapid at-line AAVX affinity HPLC: enabling process analytical technology for bioprocess development of adeno-associated virus vectors. *Biotechnol J*. 2025;20(3):e202400656. https://doi.org/10.1002/biot.202400656.
16. Wu D, Zhao X, Jimenez DA, Piszczek G. Size exclusion chromatography−mass photometry: a new method for adeno-associated virus product characterization. *Cells*. 2023;12(18):2264. https://doi.org/10.3390/cells12182264.
17. McIntosh NL, Berguig GY, Karim OA, et al. Comprehensive characterization and quantification of adeno associated vectors by size exclusion chromatography and multi angle light scattering. *Sci Rep*. 2021;11(1):3012. https://doi.org/10.1038/s41598-021-82599-1.
18. Troxell B, Tsai IW, Shah K, et al. Application of size exclusion chromatography with multiangle light scattering in the analytical development of a preclinical stage gene therapy program. *Hum Gene Ther*. 2023;34(7-8):325–338. https://doi.org/10.1089/hum.2022.218.
19. Duong T, McAllister J, Eldahan K, et al. Improvement of precision in recombinant adeno-associated virus infectious titer assay with droplet digital PCR as an endpoint measurement. *Hum Gene Ther*. 2023;34(15-16):742–757. https://doi.org/10.1089/hum.2023.014.
20. Wagner C, Fuchsberger FF, Innthaler B, Lemmerer M, Birner-Gruenberger R. Quantification of empty, partially filled and full adeno-associated virus vectors using mass photometry. *Int J Mol Sci*. 2023;24(13):11033. https://doi.org/10.3390/ijms241311033.
21. Wagner C, Fuchsberger FF, Innthaler B, et al. Automated mass photometry of adeno-associated virus vectors from crude cell extracts. *Int J Mol Sci*. 2024;25(2):838. https://doi.org/10.3390/ijms25020838.
22. Ebberink EHTM, Ruisinger A, Nuebel M, Thomann M, Heck AJR. Assessing production variability in empty and filled adeno-associated viruses by single molecule mass analyses. Mol Ther - Methods Clin Dev. 2022;27:491–501. https://doi.org/10.1016/j.omtm.2022.11.003.
23. ThermoFisher. Qubit® ssDNA assay kit. Preprint posted online March 8, 2022. Accessed October 21, 2025. https://documents.thermofisher.com/TFS-Assets%2FLSG%2Fmanuals%2FQubit_ssDNA_Assay_UG.pdf.
24. Mulagapati SHR, Parupudi A, Witkos T, et al. Size-exclusion chromatography as a multi-attribute method for process and product characterization of adeno-associated virus. Mol Ther - Methods Clin Dev. 2024;32(4):101382. https://doi.org/10.1016/j.omtm.2024.101382.
25. Imiołek M, Fekete S, Kizekai L, Addepalli B, Lauber M. Fast and efficient size exclusion chromatography of adeno associated viral vectors with 2.5 micrometer particle low adsorption columns. *J Chromatogr A*. 2024;1714:464587. https://doi.org/10.1016/j.chroma.2023.464587.
26. Cole L, Fernandes D, Hussain MT, Kaszuba M, Stenson J, Markova N. Characterization of Recombinant Adeno-Associated Viruses (rAAVs) for gene therapy using orthogonal techniques. *Pharmaceutics*. 2021;13(4):586. https://doi.org/10.3390/pharmaceutics13040586.
27. Rodenstein C, Schmid E, Markova N, Seidl A. Identification of relevant analytical methods for adeno-associated virus stability assessment during formulation development. *Microbiol Spectr*. 2025;13(8):e01806. https://doi.org/10.1128/spectrum.01806-24. -24.
28. Bee JS, Zhang Y (Zoe), Phillippi MK, et al. Impact of time out of intended storage and freeze-thaw rates on the stability of adeno-associated virus 8 and 9. *J Pharm Sci*. 2022;111(5):1346–1353. https://doi.org/10.1016/j.xphs.2022.01.002.
29. Wright JF, Le T, Prado J, et al. Identification of factors that contribute to recombinant AAV2 particle aggregation and methods to prevent its occurrence during vector purification and formulation. *Mol Ther*. 2005;12(1):171–178. https://doi.org/10.1016/j.ymthe.2005.02.021.
30. Lengler J, Gavrila M, Brandis J, et al. Crucial aspects for maintaining rAAV stability. *Sci Rep*. 2024;14(1):27685. https://doi.org/10.1038/s41598-024-79369-0.
31. Giles AR, Sims JJ, Turner KB, et al. Deamidation of amino acids on the surface of adeno-associated virus capsids leads to charge heterogeneity and altered vector function. *Mol Ther*. 2018;26(12):2848–2862. https://doi.org/10.1016/j.ymthe.2018.09.013.
32. Maruno T, Fukuhara M, Tsunaka Y, et al. Variation of VP2 stoichiometry and deamidation of VP1 during production and their impacts on the transduction efficiency of AAV vectors. *Mol Ther Methods Clin Dev*. 2025;33(4):101581. https://doi.org/10.1016/j.omtm.2025.101581.
33. Townsend JA, Li S, Sweezy L, et al. Comparative analysis of empty and full adeno-associated viruses under stress conditions by anion-exchange chromatography, analytical ultracentrifugation, and mass photometry. *J Pharm Sci*. 2025;114(2):1237–1244. https://doi.org/10.1016/j.xphs.2025.01.005.
34. Xing T, Li S, Tang S, et al. Distinct chemical degradation pathways of AAV1 and AAV8 under thermal stress conditions revealed by analytical anion exchange chromatography and LC-MS-based peptide mapping. *J Pharm Biomed Anal*. 2024;251:116452. https://doi.org/10.1016/j.jpba.2024.116452.

35. Rodriguez A, Banazadeh A, Ali A, Singh R, Zhou C. Limitation of anion exchange chromatography and potential application of hydrophobic interaction chromatography for monitoring AAV9 capsid degradation upon thermal stress. *J Pharm Sci*. 2025;114(2):983–989. https://doi.org/10.1016/j.xphs.2024.11.005.
36. Kurth S, Li T, Hausker A, et al. Separation of full and empty adeno-associated virus capsids by anion-exchange chromatography using choline-type salts. *Anal Biochem*. 2024;686:115421. https://doi.org/10.1016/j.ab.2023.115421.
37. Stahnke S, Lux K, Uhrig S, et al. Intrinsic phospholipase A2 activity of adeno-associated virus is involved in endosomal escape of incoming particles. *Virology*. 2011;409(1):77–83. https://doi.org/10.1016/j.virol.2010.09.025.
38. Girod A, Wobus CE, Zádori Z, et al. The VP1 capsid protein of adeno-associated virus type 2 is carrying a phospholipase A2 domain required for virus infectivity. *J Gen Virol*. 2002;83(5):973–978. https://doi.org/10.1099/0022-1317-83-5-973.
39. Frederick A, Sullivan J, Liu L, et al. Engineered capsids for efficient gene delivery to the retina and cornea. *Hum Gene Ther*. 2020;31(13-14):756–774. https://doi.org/10.1089/hum.2020.070.
40. Takino R, Yamaguchi Y, Maruno T, et al. Physicochemical and biological impacts of light stress on adeno-associated virus serotype 6. Mol Ther - Methods Clin Dev.. 2024;32(4):101362. https://doi.org/10.1016/j.omtm.2024.101362.
41. Evidence that ionic interactions are involved in concentration-induced aggregation of recombinant adeno-associated virus. *Mol Ther*. 2003;7(5):S348. https://doi.org/10.1016/s1525-0016(16)41343-2.
42. Nam HJ, Gurda BL, McKenna R, et al. Structural studies of adeno-associated virus serotype 8 capsid transitions associated with endosomal trafficking. *J Virol*. 2011;85(22):11791–11799. https://doi.org/10.1128/jvi.05305-11.
43. Ye X, Hu M, Hu Y, Qiu H, Li N. HDX-MS reveals pH and temperature-responsive regions on AAV capsids and the structural basis for DNA release. *Gene Ther*.. 2025:1–11. https://doi.org/10.1038/s41434-025-00539-4. Published online.
44. Potter M, Lins B, Mietzsch M, et al. A simplified purification protocol for recombinant adeno-associated virus vectors. Mol Ther - Methods Clin Dev.. 2014;1:14034. https://doi.org/10.1038/mtm.2014.34.
45. ICH Harmonised Tripartite Guideline. Stability testing:photostability testing of new drug substances and products Q1B; 1996. Accessed September 2, 2025; 1996. https://www.ich.org/.
46. Aronson SJ, Bakker RS, Moenis S, et al. A quantitative in vitro potency assay for adeno-associated virus vectors encoding for the UGT1A1 transgene. Mol Ther - Methods Clin Dev. 2020;18:250–258. https://doi.org/10.1016/j.omtm.2020.06.002.
47. Steininger T, Öttl V, Franken LE, et al. Improved recombinant adeno-associated viral vector production via molecular evolution of the viral rep protein. *Int J Mol Sci*. 2025;26(3):1319. https://doi.org/10.3390/ijms26031319.
48. Kontogiannis T, Braybrook J, McElroy C, et al. Characterization of AAV vectors: a review of analytical techniques and critical quality attributes. Mol Ther - Methods Clin Dev. 2024;32(3):101309. https://doi.org/10.1016/j.omtm.2024.101309.
49. Graf T, Naumann L, Bonnington L, et al. Expediting online liquid chromatography for real-time monitoring of product attributes to advance process analytical technology in downstream processing of biopharmaceuticals. *J Chromatogr A*. 2024465013. https://doi.org/10.1016/j.chroma.2024.465013. Published online.
50. Steppert P, Burgstaller D, Klausberger M, Tover A, Berger E, Jungbauer A. Quantification and characterization of virus-like particles by size-exclusion chromatography and nanoparticle tracking analysis. *J Chromatogr A*. 2017;1487:89–99. https://doi.org/10.1016/j.chroma.2016.12.085.
51. Zanker J, Lázaro-Petri S, Hüser D, Heilbronn R, Savy A. Insight and development of advanced recombinant adeno-associated virus analysis tools exploiting single-particle quantification by multidimensional droplet digital PCR. *Hum Gene Ther*. 2022;33(17-18):977–989. https://doi.org/10.1089/hum.2021.182.